Mapping human laryngeal motor cortex during vocalization

Nicole Eichert[1], Daniel Papp[1], Rogier B. Mars[1,2] & Kate E. Watkins[3]

[1] Wellcome Centre for Integrative Neuroimaging, Centre for Functional MRI of the Brain (FMRIB), Nuffield Department of Clinical Neurosciences, John Radcliffe Hospital, University of Oxford, Oxford, United Kingdom

[2] Donders Institute for Brain, Cognition and Behaviour, Radboud University Nijmegen, Nijmegen, The Netherlands

[3] Wellcome Centre for Integrative Neuroimaging, Department of Experimental Psychology, University of Oxford, Oxford, United Kingdom

Abbreviated title: human laryngeal motor cortex

Correspondence:

Nicole Eichert

Wellcome Centre for Integrative Neuroimaging

Nuffield Department of Clinical Neurosciences

John Radcliffe Hospital

University of Oxford

Oxford OX3 9DU

United Kingdom

Direct Line: +44)0)1865 271363

E-mail: nicole.eichert@psy.ox.ac.uk

Abstract

Human speech production requires fine neural control of the articulators and the larynx during vocalization. The representation of the larynx in the human brain is debated. Vocalizations can be elicited by stimulation of the ventral motor cortex, but neuroimaging reveals that producing vocalizations evokes activity in both a dorsal and a ventral area. We designed an fMRI study to isolate brain activity related to laryngeal activity during vocalization while controlling for breathing. We mapped the cortical motor representation of the larynx during vocalization and dissociated it from representations of supralaryngeal articulators (the lips and tongue). We also mapped the hand representation in the left hemisphere. Furthermore, we characterized the microstructure of activated cortical regions using structural and quantitative neuroimaging in individual subjects. We found two separate activations during vocalization, which are in anatomically distinct parts of the brain. Individual subjects show a consistent somatotopic arrangement of the movement-related activations. Quantifications of cortical microstructure suggest that the dorsal, but not the ventral larynx area, is located in primary motor cortex as indexed by high myelin content and thicker cortex. It remains unclear, however, whether and how these two brain areas differentially contribute to laryngeal motor control.

Keywords

- Functional MRI
- Larynx
- Myelin
- Quantitative MRI
- Speech

1. Introduction

The voluntary control of highly complex speech movements is regarded as one aspect of behavior that is unique to humans (Fitch 2017). Speech production requires the fine coordination of a large number of muscles to control the supralaryngeal articulators, respiration, and the vocal folds in the larynx during voice production (Jürgens 2002). In addition to its role as main source of vocal sound production, the larynx is implicated in various biological functions such as protection of the airways and swallowing (Ludlow 2005). Several pairs of intrinsic and extrinsic muscles connect the laryngeal cartilages with each other and to the skeleton. During vocalization, these muscles are controlled in a complex fashion, so that the tension in the vocal folds allows them to be set into vibration as air from the lungs passes through them. Several lines of evidence showed that the ventral part of the precentral gyrus in the human brain is involved in speech motor control (Bohland and Guenther 2006; Ackermann et al. 2014). The question as to which brain areas specifically control laryngeal activity during vocalization, however, remains debated.

Nearly 100 years ago, direct cortical stimulation of the ventral portion of the precentral gyrus in the human brain was shown to elicit vocalization (Foerster 1936; Penfield and Boldrey 1937). In more recent times, functional brain imaging studies show highly inconsistent results when mapping laryngeal activity during vocalization (see Belyk & Brown, 2017 for review). Several studies report activity evoked by vocalization in both a ventral portion of the precentral gyrus located close to the Sylvian fissure and in a more dorsal portion of central sulcus and precentral gyrus (Terumitsu et al. 2006; Galgano and Froud 2008; Olthoff et al. 2008; Grabski et al. 2012). Some studies report vocalization-evoked activity in the dorsal location only (Sörös et al. 2006;

Brown et al. 2008; Kleber et al. 2013; Belyk and Brown 2014; Belyk et al. 2018). Only a few studies specifically isolated laryngeal activity during voice production by contrasting it with supralaryngeal articulation (Sörös et al. 2006; Terumitsu et al. 2006; Brown et al. 2009; Grabski et al. 2012), but the results were inconsistent across studies.

Another line of evidence comes from direct neurophysiological recordings from the cortical surface using implanted high-density electrode arrays in patients being prepared for epilepsy surgery. These studies also show activity in both a dorsal and a ventral area during speech production (Bouchard et al. 2013; Chang et al. 2013; Toyoda et al. 2014; Breshears et al. 2015; Dichter et al. 2018). Interpretation of electrocorticography (ECoG) studies, however, is inherently limited due to the typically small sample size and due to potential neurological abnormalities in the patients' brains.

In addition to these inconsistent results, a potential confound in several studies mentioned above is breathing. Voice production and exhalation functionally interact during speech production and volitional expiration has been shown to activate motor areas that are located close to the putative dorsal laryngeal area (Ramsay et al. 1993; McKay et al. 2003). Several previous studies, however, did not control for breathing (e.g. Brown et al., 2008; Sörös et al., 2006). Those studies that specifically studied vocalization and breathing found largely overlapping activity during both conditions and a contrast showed no difference in motor cortex indicating that the activity was not specific to larynx activity (Loucks et al. 2007; Simonyan et al. 2009).

In addition to a lack of control for confounds such as breathing and supralaryngeal articulation, most neuroimaging studies mentioned above did not assess individual differences in the activation patterns. It is common to report group-level cluster-corrected results following volumetric nonlinear image registration of task-activation maps. Interpreting group-level results, however, might obscure subject-specific features and inter-individual variability, which limits sensitivity and functional resolution (Bennett and Miller 2010; Nieto-Castañón and Fedorenko 2012; Bouchard et al. 2013; Woo et al. 2014). This lack of individual detail might have caused a failure to detect one of the larynx areas in previous studies. Moreover, averaging of small sample sizes with high variability, as often performed in ECoG studies, can show two larynx areas, even when individual patients show activity in only one of the areas (Bouchard et al. 2013).

Comparisons of human brains and those of other primates indicate strong species differences in the neural organization underlying laryngeal control during vocalization (Ackermann et al. 2014; Simonyan 2014; Kumar et al. 2016). Most notably, the location of the proposed human dorsal larynx area in primary motor cortex is more dorsal-posterior than the non-human primate homolog, which is in a ventral premotor cortex area (Leyton and Sherrington 1917; Hast et al. 1974; Jürgens 1974; Simonyan and Jürgens 2002; Coudé et al. 2011). Furthermore, as noted above, numerous studies indicate that there might be two distinct representations of the larynx in the human brain.

These various findings have led to the proposal of an evolutionary 'duplication and migration' hypothesis that the larynx motor cortex comprises two structures located dorsally and ventrally in the human brain (Belyk and Brown, 2017; Jarvis, 2019; reviewed in Mars et al.,

2018). This theory proposes that the dorsal larynx area is a uniquely human brain area that evolved in primary motor cortex due to our especially high demands on laryngeal motor control. The ancestral primate larynx area in premotor cortex is presumed to be homologous to the human ventral larynx area, which migrated posteriorly, potentially into human primary motor cortex.

The cytoarchitectonic properties of the two larynx areas and their distinct functional contributions, however, remain unknown to date. Describing the underlying anatomical parcels can inform hypotheses about the cytoarchitectonic properties and the functional relevance of these areas. A myeloarchitectonic approach, which has also become available for neuroimaging, enables visualization of borders of the primary sensory-motor area based on, for example, cortical myelin content and cortical thickness (Fischl and Dale 2000; Glasser and van Essen 2011; Lutti et al. 2014).

This study thus sought to determine the anatomical location of larynx-related neural activity in individual subjects and to characterize the cortical structure underlying these areas. Our experimental design aimed to isolate brain activity related to voice production by controlling for breathing-related movements and movements of articulators. In one task, we identified the (supralaryngeal) articulation and the (laryngeal) vocalization component of speech during syllable production using a factorial design described in a previous study (Murphy et al. 1997). We refer to the latter ‘vocalization’ component as an index for laryngeal activity during voice production, while other studies have referred to it as ‘phonation’ or ‘voicing’. In a second task, we localized the separate neural representations of lip, tongue and larynx using highly controlled basic movements, while breathing movements were matched across conditions.

In order to characterize the microstructural properties underlying the larynx areas, we compared their myelin content and cortical thickness derived from structural and quantitative MRI measurements. These quantifications give an indication of the type of cortex underlying the activated area, to inform our knowledge about the organization of human larynx motor cortex.

2. Materials and Methods

Subjects

20 subjects (12 females, 18 – 40 years, 5 left-handers) took part in the study. All subjects were self-reported native English speakers (two were raised bilingually and three were fluent in a second language), and had no history or diagnoses of speech disorders. All had normal hearing, normal or corrected-to-normal vision, and no neurological impairments. The study was approved by the Central University Research Ethics Committee (CUREC, R55787/RE001) in accordance with the regulatory standards of the Code of Ethics of the World Medical Association (Declaration of Helsinki). All subjects gave informed consent to their participation and were monetarily compensated for their participation.

Experimental design and task

Subjects practiced all tasks outside the scanner to be sure they understood the task requirements. Articulator movements and vocalizations as well as breathing were demonstrated by the experimenter and practiced until the subjects performed them as required.

Task 1 - syllable production task

Subjects were instructed to produce the utterance "/la leɪ li la leɪ li/" in four different conditions: speaking (overt speech), supralaryngeal articulation only (silent mouthing), overt vowel sound production of vowel /i/ but no articulation (vowel production) and thinking (covert speech). For all conditions, the breathing pattern was explicitly instructed using the fixation symbol on the screen. Subjects were instructed to inhale for 1.5 s (fixation was a square) and exhale for 4 s (fixation was a cross). In the 'overt speech' condition, subjects said the utterance once during exhalation. In the 'silent mouthing' condition, subjects articulated the utterance using their tongue without making a sound. They were instructed not to whisper as this would involve laryngeal motor activity. During the 'vowel production' condition, subjects produced the /i/ vowel six times. The 'covert speech' condition required subjects to produce the utterance covertly while maintaining the breathing pattern. Subjects were instructed to keep their mouth slightly open during the whole session and to keep the jaw relaxed.

Each condition was performed in blocks lasting 22 s, which corresponded to four repetitions of the breathing cycle. Each block was followed by a rest period of 8 s with normal breathing. The rest period allowed the subjects to relax their breathing patterns and to maintain a

comfortable respiratory state. The four conditions were presented in a fixed pseudo-random order following a balanced Latin-square design wherein each condition was repeated five times; each condition followed and preceded each of the other conditions once and the same condition was not presented consecutively.

Task 2 - basic functional localizer

There were three task conditions: production of the vowel sound /i/, lip protrusion, tongue retraction, and a baseline 'breathing only' condition. The vowel /i/ was chosen because it is a natural and familiar sound that requires laryngeal movement during vocalization, but involves minimal movement of the jaw muscles, lips and pharyngeal part of the tongue (Grabski et al. 2012). Articulator movements and vowel production were repeated at a rate of approximately 1 - 2 repetitions/s. Subjects were instructed to keep the movement rate constant throughout the scan for all movement types. Breathing instructions, task timing and randomization of the blocks were the same as described for task 1, except that each condition was repeated four times during the scan run. During the scanning session, this task was performed prior to the syllable production task.

Hand localizer

In between the two tasks involving vocalizations, the subjects performed a phonological and semantic judgement task, which involved button presses to indicate responses. The task was

used here only to localize the hand area in the left hemisphere; the language task data are not reported.

MRI Data Acquisition

MRI data were obtained at the Oxford Centre for Human Brain Activity (OHBA) using a 3-T Siemens Prisma scanner with a 32-channel head coil. Two structural images of the whole brain were acquired; a T1w image (MPRAGE sequence; 1 mm^3 isotropic resolution, TR = 1900 ms, TE = 3.97 ms, TI = 905 ms, 8° flip angle, bandwidth = 200 Hz/pixel, echo spacing = 9.2 ms, FOV = 192 × 192 × 174 mm^3) and a T2w image (SPACE turbo-spin-echo sequence; 1 mm^3 isotropic resolution, TR = 3200 ms, central TE = 451 ms, variable flip angle, bandwidth = 751 Hz/pixel, echo spacing = 3.34 ms, echo train duration = 919 ms, Turbo Factor = 282, FOV = 256 × 256 × 176 mm^3, GRAPPA acceleration factor 2).

For task fMRI, whole-head T2*-weighted echo-planar images (TE = 30 ms) were acquired using multiband sequence (factor 6, TR = 0.8) at 2.4 mm^3 isotropic resolution. Task fMRI parameters were adopted from the ABCD study (https://biobank.ctsu.ox.ac.uk/crystal/docs/brain_mri.pdf, Casey et al., 2018). Two task fMRI scans were conducted lasting 8 min (600 volumes, task 2) and 10 min (750 volumes, task 1). In between the two tasks, subjects performed a phonological and semantic judgement task for 9 min, which did not involve vocalization.

Furthermore, a multiparameter mapping (MPM) protocol was acquired (Weiskopf et al. 2013; Lutti et al. 2014). Proton density-weighted (MPM_{PDw}), magnetization transfer-weighted

250 (MPM_{MTw}) and T1-weighted (MPM_{T1w}) images were acquired using a tailored pulse sequence
251 (1 mm^3 isotropic resolution, FOV = 256 × 224 × 176 mm^3, TR = 25 ms, bandwidth = 488
252 Hz/pixels, first TE/echo spacing = 2.3/2.3 ms, 6° flip angle (MPM_{PDw}, MPM_{MTw}) or 21° (MPM_{T1w}),
253 slab rotation = 30°, and number of echoes = 8/6/8 (MPM_{PDw}/MPM_{MTw}/MPM_{T1w} respectively),
254 GRAPPA acceleration factor 2 × 2, 40 reference lines in each phase encoded direction.
255
256 Quantitative R1 (= 1 / T1) maps were estimated from the MPM_{PDw} and MPM_{T1w} images
257 according to the model developed by Helms et al. (2009) which was extended by including a
258 correction for radio frequency transmit field inhomogeneities (Lutti et al. 2010) and imperfect
259 spoiling (Preibisch and Deichmann 2009). Regression of the log-signal from the signal decay
260 over echoes across all three MPM contrasts was used to calculate a map of R2* (= 1 / T2*)
261 (Weiskopf et al. 2014). The transmit field map was calculated using a 3D echo-planar
262 imaging (EPI) spin-echo (SE)/stimulated echo (STE) method (Lutti et al., 2012, 2010; FOV = 256
263 × 192 × 192 mm^3, matrix = 64 × 64 × 48 mm^3, TE = 39.06, mixing time = 33.8 ms, TR = 500 ms,
264 nominal α varying from 115° to 65° in steps of 5°, acquisition time 4 min 24 s) and was
265 corrected for off-resonance effects using a standard B0 field map (double gradient echo FLASH,
266 3 × 3 × 2 mm^3 resolution, whole-brain coverage). The MPM parameter maps took
267 approximately 20 minutes to acquire. The total duration of the scanning session was
268 approximately 1.5 h.
269
270 Physiological recordings were carried out throughout scanning using a respiratory belt to
271 measure the breathing pattern and a pulse oximeter to monitor the heart rhythm.
272 Physiological data were recorded using a Biopac MP150 (Biopac, Goleta, CA, USA) at a sampling
273 frequency of 500 Hz. Subjects wore ear-plugs and MRI-compatible head phones (OptoActive-

II, Optoacoustics Ltd, Moshav Mazor, Israel), which reduced scanner noise using electrodynamic noise-cancelling. At the beginning of the scanning session, the headphones were calibrated and noise-cancelling performance was further monitored throughout the session. Prior to each functional scan the attenuation algorithm 'learned' the scanner noise for 16 s. During the two tasks involving vocalizations, subjects were audio-recorded using a MRI-compatible microphone with noise cancelling (Dual Channel FOMRI-III, Optoacoustics Ltd, Moshav Mazor, Israel) at a sampling rate of 22,050 Hz.

Behavioral data analysis

The subjects' vocal behavior for the tasks was assessed using the audio recordings. The breathing patterns during the task blocks recorded using the Biopac were inspected visually to verify that subjects complied with the breathing instruction. Individual breathing traces were cropped into segments of 30 s, which consist of 22 s of instructed breathing during the task block and 8 s of subsequent rest period with normal breathing.

Structural MRI analysis

T1w and T2w scans were pre-processed using the HCP-pipeline (Glasser et al. 2013) cloned from the 'OxfordStructural' - fork (https://github.com/lennartverhagen/Pipelines). The processing pipeline includes anatomical surface reconstruction using FreeSurfer and automatic assignment of neuroanatomical labels (Fischl 2012; Jenkinson et al. 2012). The

T2w image was registered to the T1w image using FSL's FLIRT using spline interpolation (Jenkinson et al. 2002).

The image of the T1w scan was divided by the image of the T2w scan to create a T1w/T2w-ratio image. The T1w/T2w-ratio was mapped onto the native midthickness surface and then resampled to the 164k standard (fs_LR) surface mesh (approx. 164.000 vertices per hemisphere) using Workbench Command (www.humanconnectome.org/software/connectome-workbench.html). Mapping was performed with the `-volume-to-surface-mapping` command using the `-myelin-style` option. This T1w/T2w map has been shown empirically to correlate with cortical myelin content (Glasser and van Essen 2011; Glasser et al. 2014). In addition to T1w/T2w myelin maps, the HCP-pipeline provides automatic generation of cortical thickness surface maps.

MPM parameter maps were reconstructed and pre-processed using the hMRI-toolbox (Tabelow et al. 2019) embedded in the Statistical Parametric Mapping framework (SPM12, Wellcome Trust Centre for Neuroimaging, London, UK). For one subject, MPM data were excluded due to motion-induced blurring. MPM_{MT}, MPM_{R1} and MPM_{R2*} maps were registered to the MPRAGE T1w scan using FLIRT rigid-body transformation and then mapped to the surface using the same steps as for the T1w/T2w myelin map. The three MPM parameter maps have been shown to correlate to different degrees with myelin content in white matter, subcortical structures and grey matter (Draganski et al. 2011; Callaghan et al. 2014; Lutti et al. 2014; Bagnato et al. 2018). Finally, one step of surface-based smoothing (FWHM = 4 mm) was applied to the five surface maps of interest - T1w/T2w map, three MPM parameter maps and cortical thickness map.

fMRI data analysis

Functional MRI data processing was carried out using FEAT (FMRI Expert Analysis Tool) Version 6.00, part of FSL (FMRIB's Software Library, www.fmrib.ox.ac.uk/fsl). The following pre-statistics processing was applied: motion correction using MCFLIRT (Jenkinson et al. 2002); non-brain tissue removal using BET (Smith 2002); spatial smoothing using a Gaussian kernel (FWHM = 5 mm); grand-mean intensity normalization of the entire 4D dataset by a single multiplicative factor; low-frequency drifts were removed using a temporal high-pass filter with a cut-off of 90 s for all three tasks. Motion corrected images were unwarped using a fieldmap and PRELUDE and FUGUE software running in FSL (Jenkinson 2003). Registration to the high resolution structural scan and standard 2 mm MNI-152 template was carried out using FLIRT (Jenkinson and Smith 2001; Jenkinson et al. 2002). Registration from high resolution structural to standard space was then further refined using FNIRT nonlinear registration (Andersson et al. 2007).

Time-series statistical analysis was based on a general linear model (GLM) implemented in FILM with local autocorrelation correction (Woolrich et al. 2001). Standard motion correction parameters and individual volumes that were motion outliers, determined using fsl_motion_outliers, were included as separate regressors at the first level for each subject.

For the syllable production task (task 1), the conditions were analyzed in a factorial model that allowed to separate out the (supralaryngeal) articulation and the (laryngeal) vocalization

346 component of the task. Brain activity associated with the control of articulation was defined as
347 ('overt speech' *minus* 'vowel production') *plus* ('silent mouthing' *minus* 'covert speech') and
348 the main contrast for vocalization was derived by the contrast ('overt speech' *minus* 'silent
349 mouthing') *plus* ('vowel production' *minus* 'covert speech'). The rest blocks served as the
350 baseline condition and were not modelled in the GLM.
351
352 For the basic localizer task (task 2), activity during each condition was assessed relative to the
353 'breathing only' condition, while rest blocks with normal breathing served as baseline (i.e. they
354 were not modelled in the GLM). Note that in both tasks, the rest blocks served as baseline, but
355 the contrasts of interest were computed relative to conditions that included the same
356 breathing instruction. Results of all individual task conditions relative to the rest condition are
357 reported in a supplementary figure (Figure S1). For the hand localizer task, we derived a
358 contrast of all conditions involving button presses relative to the resting baseline.
359
360 To obtain volumetric group average maps, each individual's statistical maps were transformed
361 to standard space (MNI152) using a nonlinear registration. Volumetric group mean activation
362 maps were obtained using mixed effects in FLAME (FMRIB's Local Analysis of Mixed Effects,
363 Woolrich, Behrens, Beckmann, Jenkinson, & Smith, (2004), Stage 1 only), where subjects are
364 treated as random effects. Group-level *z*-statistic images were thresholded using an
365 uncorrected voxel-wise threshold of $z > 3.5$ ($p < 0.001$). Volumetric group-level result figures
366 are focused, i.e. centered, on the voxel of maximal *z*-value within the central somatomotor
367 strip. For the vocalization contrast (task 1) and the vowel production condition (task 2), we
368 generated two separate results figures focused on the dorsal and the ventral larynx area.
369

Surface group count maps

In addition to volume-based analysis, task MRI activations were assessed using surface-based analyses. Each subject's *z*-statistic images were thresholded at $p < 0.05$ (corrected voxel-wise, based on data smoothness and the RESEL count) and mapped onto the individual's native midthickness surface using the '-ribbon-enclosed' option in wb_command `-volume-to-surface-mapping`. To derive group-level activation maps, all individual subject maps were resampled to the 32k standard (fs_LR) mesh based on the FreeSurfer registration, binarized and then summed at each vertex to create a group count map (Barch et al. 2013). The group count maps are shown on an inflated average brain surface, thresholded at $n > 4$ subjects.

ROI definitions to extract activation maxima

In order to assess intra-individual variability of the fMRI results, we derived the location of individual activation maxima for hand, lip, and tongue movement, and larynx activity during vocalization. Activation maxima were derived in both hemispheres in volume space using anatomically defined ROIs. An individual example of the volumetric ROIs is shown in the Supplementary Material (Figure S3). For hand (left hemisphere only), lip, and tongue movement, we used the central sulcus as a volumetric ROI to extract the maximum voxel. The ROI was defined using FreeSurfer's automatic volumetric labelling based on the Destrieux Atlas.

For the vocalization contrast from the syllable production task, which indicates laryngeal activity during voice production, we derived two separate activation maxima: one located in the dorsal area and one in a ventral area of the central sulcus. To account for additional articulation of the tongue during the syllable production task, a spherical ROI (7 voxels diameter) around each individual's maximum voxel from the tongue movement localizer was masked out from the *z*-statistics image of the vocalization contrast prior to extracting the maximal voxel.

For the dorsal larynx ROI, we used a dorsally and ventrally cropped section of the central sulcus in volume space (coordinates in MNI space: $z = 50$ to $z = 30$). The ventral larynx ROI was derived manually based on individual anatomy in surface space to ensure that the ROI did not overlap with unrelated brain areas such as the subjacent auditory cortex in the temporal lobe or inferior frontal cortex located anteriorly. A liberal surface ROI was drawn on the individual's midthickness surface covering the ventral part of the central sulcus and adjacent gyri. Anteriorly, the ROI was delineated by the inferior portion of the precentral sulcus and posteriorly the ROI spanned the postcentral gyrus. If present, the lateral portion of the ascending sulcus in subcentral gyrus was included within the ROI. The dorsal limit of the ROI was defined by a horizontal line across the gyrus at the level of the usual location of the posterior ramus of the inferior precentral sulcus. The ventral larynx surface ROI was converted into a volumetric ROI covering the underlying cortical ribbon using wb_command.

Individual surface activation maxima

Individual volumetric ROIs were linearly transformed from FreeSurfer's anatomical to functional space of the respective task fMRI scan. Within the ROI, the voxel of maximal intensity was determined from the *z*-statistics image. It should be noted that for some subjects this local maximum did not achieve the corrected voxel-wise threshold for the individual dataset (left hemisphere: hand $n = 3$, dorsal larynx $n = 6$, ventral larynx $n = 5$; right hemisphere: dorsal larynx $n = 5$, ventral larynx $n = 4$). Using a lower uncorrected threshold is justified given our goal to visualize and assess spatial variability of the activation maxima. For visualization and further analysis, the activation maxima were mapped to the individual's native midthickness surface, resampled to the 32k standard (fs_LR) surface mesh using the FreeSurfer registration and then smoothed (FWHM = 1 mm) and binarized to form a small circular patch.

We determined the within-subject reliability of activation maxima during vocalization and tongue movement by comparing them to the location of activation maxima during vowel production (from the basic localizer task) and articulation (from the syllable production task). Maxima for these contrasts were derived as described above using the same ROIs: Central sulcus for articulation; dorsal and ventral ROI for vowel production. Then, we computed the geodesic distance on the individual's native midthickness surface for pairs of maxima in central sulcus (tongue and articulation contrast) and in dorsal and ventral ROI (vocalization and vowel production contrast). Due to the irregular spacing of mesh vertices on the native surface, the computed geodesic distance are not multiples of the functional scan voxel size.

Cortical surface features at activation peaks

We described the cortical microstructure at the individual activation peaks based on different surface measures. In order to assess cortical myelin content, we used the T1w/T2w map and the MPM parameter maps (MPM_{MT}, MPM_{R1} and MPM_{R2*}). We extracted the mean value for each individual subject's surface map within the area defined by the circular patch around the vertex of maximal activation for hand, lip, tongue, dorsal larynx and ventral larynx area, i.e. at the peaks shown in Figure 4. In order to account for the different ranges in intensities and to allow direct comparison of the maps, we computed *z*-scores based on the distribution of individual values in each map and each ROI. We assessed the differences in *z*-scores across the different ROIs using a linear mixed effects analyses as implemented in R's *lmer* function (Bates and Sarkar (2007), Core Team and Foundation for Statistical Computing). The model included fixed effects for ROI (dorsal larynx, lip, tongue, ventral larynx), hemisphere (left, right) and map (T1w/T2w, MPM_{MT}, MPM_{R1}, MPM_{R2*}) and random effects for subject. A Shapiro-Wilk test revealed a normal distribution of the data at a significance level of $p > 0.001$.

In addition to cortical myelin content, we also quantified cortical thickness values at the same individual surface peaks. To increase sensitivity of the quantification described above, we excluded activation maxima that were located in a part of cortex with lower cortical thickness and thus likely to be activity in somatosensory rather than motor cortex (Fischl and Dale 2000). We used a heuristic lower threshold of 2 mm to exclude sensory activation maxima and then re-ran the statistical evaluation of myelin-values described above. A linear mixed effects analysis for the fixed effects of ROI and hemisphere and random subject effects was performed to assess cortical thickness values after exclusion of the sensory activation maxima.

In order to further characterize the differences in myelin content across the ROIs, we used an additional quantification: We computed the pair-wise Manhattan distance across the ROIs based on a vector of the four raw (i.e. non-*z*-transformed) values in each subject after excluding the sensory activation maxima. The differences across ROIs were visualized in form of a dissimilarity matrix, where we averaged Manhattan distances within each ROI first across subjects and then across hemispheres.

A linear discriminant analysis (LDA) was run to explore which combination of *z*-transformed surface features (T1w/T2w, MPM_{MT}, MPM_{R1}, MPM_{R2*}), best discriminated the ventral from the dorsal larynx area after excluding sensory activation maxima. The parameters of the LDA were estimated using a singular value decomposition with no shrinkage.

3. Results

We acquired fMRI data in 20 subjects during performance of two tasks: (1) a syllable production task required subjects to produce "/la leɪ li la leɪ li/" overtly, mouthed silently, and covertly, and to produce the vowel /i/, (2) a basic localizer task required subjects to make small repetitive movements of the lips, tongue and larynx (vowel production); an additional task was used as functional localizer for movement of the right hand.

Auditory recordings

All subjects vocalized as instructed during the conditions that involved vocalizations in both tasks. In all other conditions, subjects remained silent, as instructed.

Breathing during vocalization tasks

We recorded the breathing traces using a breath belt during both vocalization tasks to confirm that the breathing patterns were comparable across different conditions (Figure 1). As expected for all conditions in both tasks, four breathing cycles were visible in the first 22 s, during which breathing was instructed. Note that in one subject, where an extension of the breathing belt was used, the breathing trace differed in overall shape, but the breathing cycles were still visible. Examination of these figures shows that the shape of the trace and variability were similar across all conditions, but some differences were observed. For example, in the vowel production condition of the basic localizer task (task 2; Figure 1B), exhalation was more gradual and less rapid than in the other four conditions. All four conditions in the syllable production task (Figure 1A) showed a more gradual exhalation pattern than in the basic localizer task (Figure 1B).

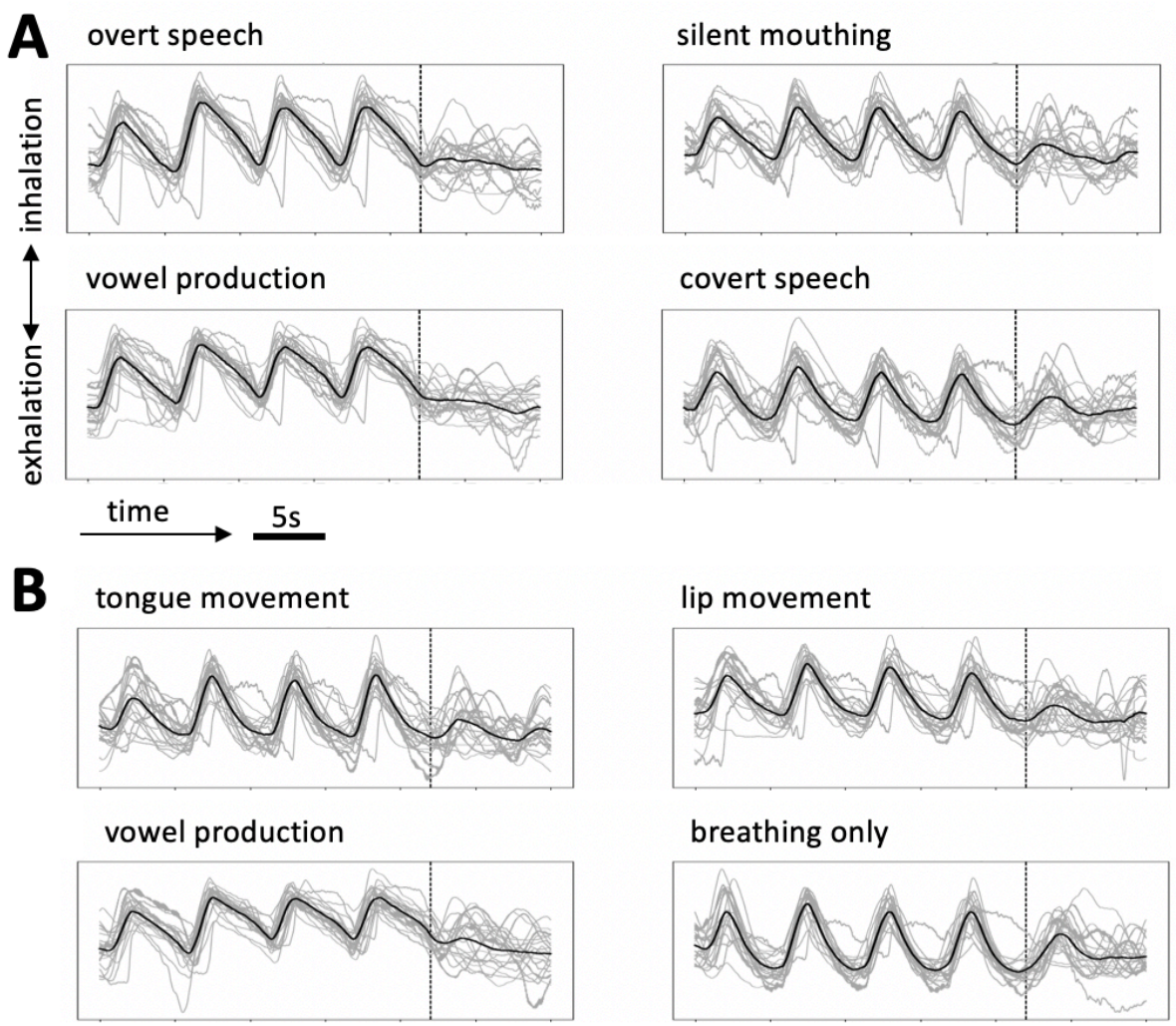

Figure 1 - Breathing patterns. **A**: Breathing traces during syllable production (task 1) (black line: group mean after normalizing all individual breathing traces to the same amplitude*, n = 20*, grey lines: average traces for individual subjects). The dashed vertical line indicates the end of the 22 s task block and the beginning of the 8 s rest block. **B**: Breathing during the basic localizer task (task 2).

Syllable production task (task 1)

Syllable production task - Volumetric results

We localized the cortical areas for movement control of (supralaryngeal) articulation and (laryngeal) vocalization during syllable production (Figure 2**A**). Brain areas involved in articulation were located in the mid-portion of the central gyrus. Note that in the articulation contrast we also found spurious activation activity in prefrontal white matter, which we presumed was induced by task-correlated movement.

The main contrast for vocalization showed activity in two somatomotor areas in both hemispheres: one located within the precentral sulcus, and a second located in a more anterior-ventral area. Portions of the superior temporal gyrus were also activated during vocalization. This is presumed to reflect auditory perception of self-generated vocalizations. The dorsal and ventral activations were separate and did not appear to be connected.

Vocalization and articulation also activated areas in cerebellum and SMA in a somatotopic fashion. Group-level volumetric results for cerebellum and SMA in both functional tasks are described in the Supplementary Material (Figure S2). In SMA, one single representation for laryngeal activity during vocalization was observed, while in cerebellum, two distinct representations were found.

Syllable production task - Surface results

Group count maps of the syllable production task projected to the surface showed that several vertices in the mid-portion of the central sulcus were commonly activated during articulation in 19 out of 20 subjects (Figure 2**B**). The group count map for vocalization showed separate

539 dorsal and ventral areas robustly activated across the group. For the vocalization contrast,
540 there was greater variability in the exact location of activity above threshold and the areas
541 activated in individuals were smaller than for the articulation contrast. This resulted in less
542 overlap of activated vertices for the vocalization group maps. For some subjects, vocalization-
543 induced activity did not reach significance in relevant brain areas, which also resulted in lower
544 values in the count map.

545

546

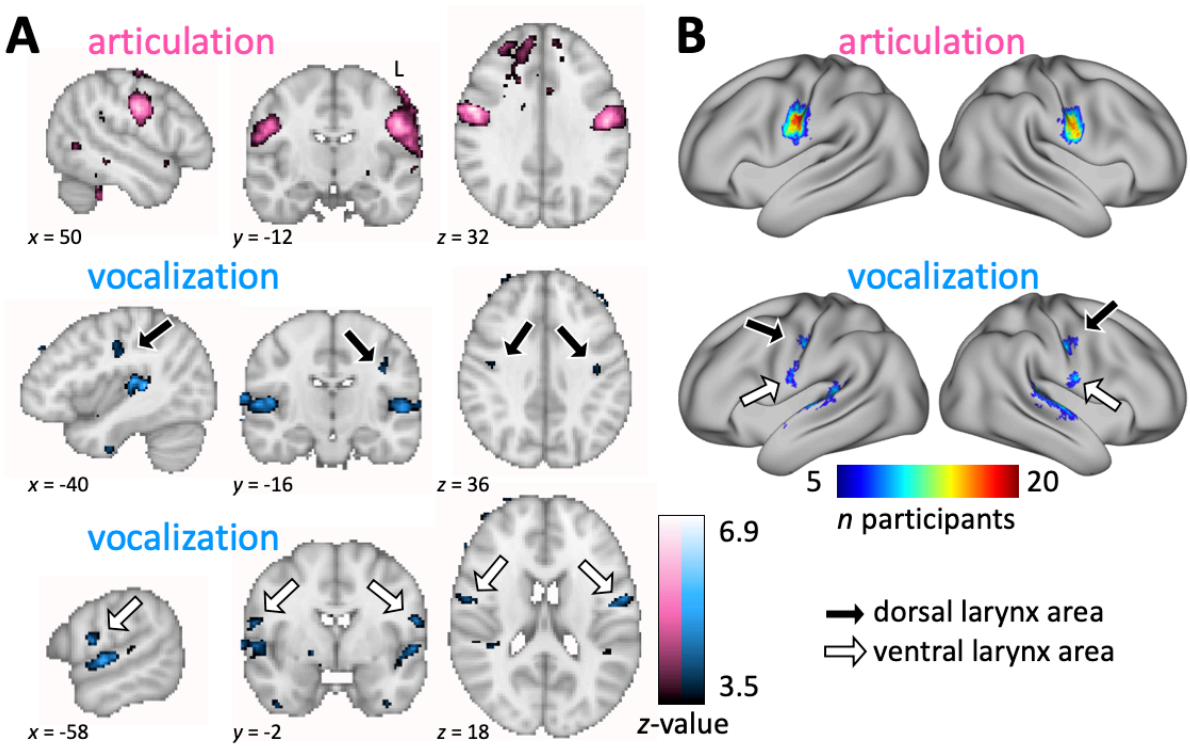

547

548 Figure 2 – Syllable production task. **A**: Group activation maps showing areas activated during articulation
549 and vocalization (voxel-wise threshold $z > 3.5$, $n = 20$). For the vocalization contrast (blue), both a dorsal and
550 a ventral area are shown in separate panels. Black arrow: dorsal larynx area; white arrow: ventral larynx
551 area. **B**: Surface group count maps of the same conditions. Individual surface maps were thresholded at $p <$
552 0.05 (corrected voxel-wise), binarized and resampled onto the fs_LR surface. These were summed across
553 the group of 20 subjects and thresholded at $n > 4$. Note: in both analyses, vocalization also resulted in

activation of the superior temporal gyrus, presumably reflecting auditory stimulation due to hearing oneself vocalizing.

Basic localizer task (task 2)

Basic localizer task - Volumetric fMRI results

We found distinct activation peaks for movement control of the tongue, the lips, and for laryngeal activity during vowel production within the mid-portion of the precentral gyrus (Figure 3A). In general, the activation maps in precentral gyrus followed the predicted somatotopic organization with the tongue representation more ventral than the lip representation in both hemispheres (Penfield and Rasmussen 1950; Grabski et al. 2012; Carey et al. 2017). The location of the activity during tongue movement overlapped with the result of the articulation contrast in the syllable production task; as previously, we found spurious activity in the prefrontal lobe white matter that we presume is movement related.

Vowel production induced activity bilaterally in a precentral/central dorsal area, a ventral area anterior to the central sulcus, and in superior temporal cortex. As for the syllable production task, this latter activity was presumed due to hearing oneself. In this group average map, and at the statistical threshold used, the dorsal and ventral areas appeared to be connected, with residual activity along the ventral central sulcus.

578 *Basic localizer task - Surface results*

579

580 Group count maps of the basic localizer task projected to the surface revealed the same
581 somatotopic activity pattern as seen in the volumetric results for group average activity (Figure
582 3**B**). The tongue condition showed highly consistent activation in the mid-portion of the central
583 sulcus during articulation (maximum overlap was achieved for all 20 subjects). The result for
584 tongue movement was highly similar to the result of the articulation contrast, which is in line
585 with the volumetric results. Complete overlap of activated vertices was not achieved for the
586 lip condition, but the activated area was still highly consistent across subjects (maximum: 15
587 subjects).

588

589 For the vowel production condition, the group count maps show a dorsal and a ventral cluster,
590 similar to the pattern seen during the vocalization contrast (task 1). The dorsal cluster extended
591 from the central sulcus to the precentral gyrus. We presumed that this dorsal precentral
592 activity, but not the sulcal activity, is a residual breathing-related effect, because it overlaps
593 with activity from the 'breathing only' condition (see Figure S1). The ventral cluster appeared
594 to extend into an area where we expected tongue activity, and may reflect residual tongue
595 activity during vowel production. In contrast to the volumetric results for the group averaged
596 activity, the count maps based on individually thresholded activation maps show the dorsal
597 and ventral areas activated by vowel production to be clearly separate.

598

599 As described above for the vocalization contrast, the values in the group count maps for vowel
600 production indicate that the location of this activity is less consistent than for the other
601 conditions; the area activated during vocalization is also smaller ,both dorsally and ventrally,

than for the articulators. The highest overlap was achieved in the right dorsal larynx representation in 11 subjects.

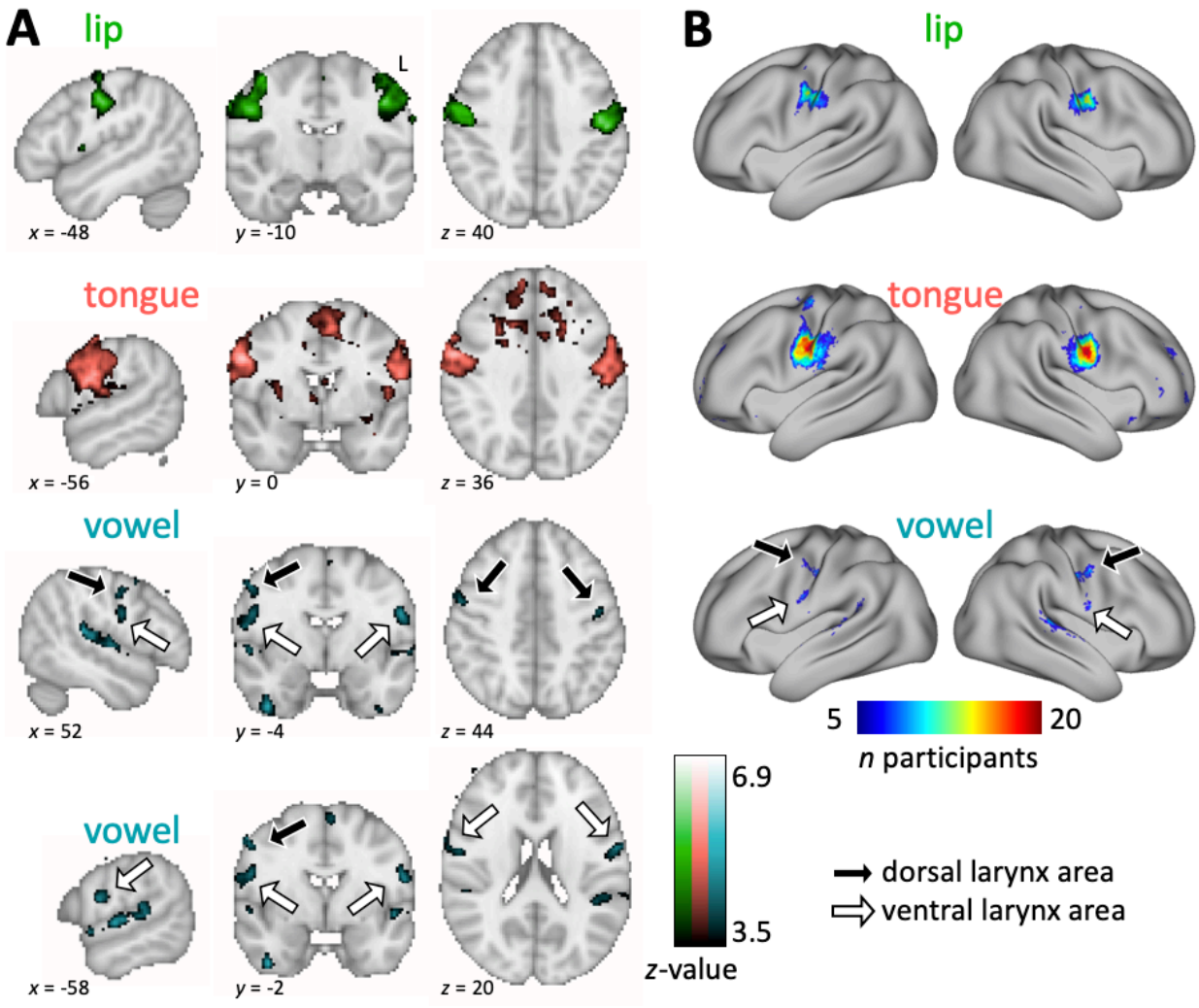

Figure 3 – Basic localizer task. **A**: Group activation maps showing areas activated during lip and tongue movement and during vowel production (vowel-wise threshold $z > 3.5$, $n = 20$). For the vowel production condition (turquoise), both a dorsal and a ventral area are shown in separate panels. Black arrow: dorsal larynx area; white arrow: ventral larynx area. Colored statistical maps were superimposed on the MNI-152 template and coordinates are provided in MNI space. L – left hemisphere shown on right side of image. **B**: Surface group count maps of the same conditions. Individual surface maps were threshold at $p < 0.05$ (corrected voxel-wise), binarized and resampled onto the fs_LR surface. These were summed across the group of 20 subjects and thresholded at $n > 4$.

Individual surface activation maxima

In order to characterize the variability of brain activity across subjects, we derived individual activation peaks for the hand movement (based on the hand-localizer, only in the left hemisphere), lip and tongue movement (based on the basic localizer task) and vocalization (based on the syllable production task). The vocalization contrast was used to localize the representation of the larynx in a dorsal and a ventral area. Figure 4 shows the distribution of individual activation peaks on an inflated brain surface. Overall, the location of the peaks for the different movement types is highly consistent with similar cross-subject variability. For the ventral larynx area, particularly in the left hemisphere, however, the location of the maxima appears to be more variable.

Within-subject reliability of the activation maxima across the two tasks was compared for 'vocalization' and 'vowel production' in both dorsal and ventral larynx area as well as for 'articulation' and 'tongue movement'. Reliability was high with a median distance across subjects of less than 10 mm for the three ROIs in both hemispheres.

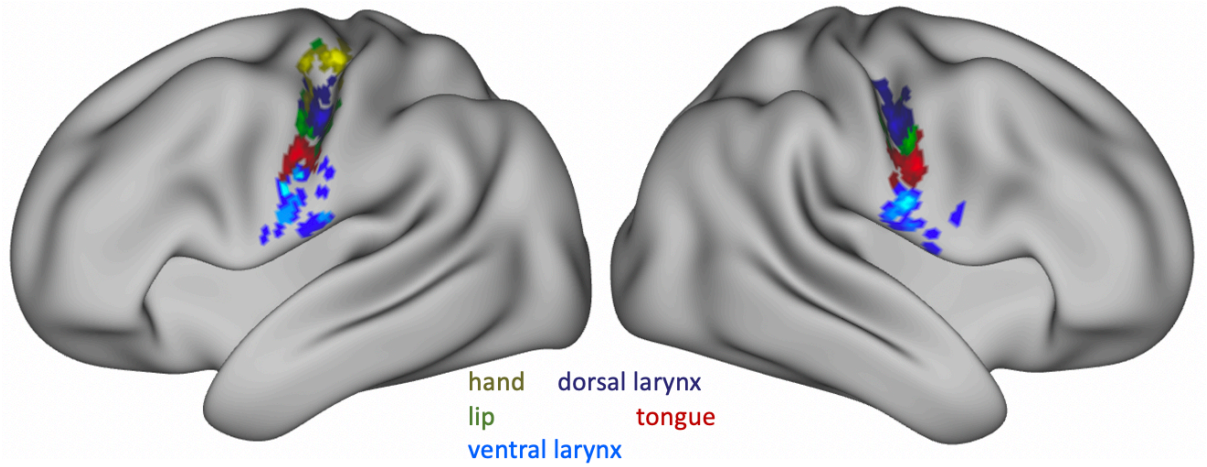

Figure 4 – Individual activation maxima. Overlay of individual activation maxima derived for hand movement (only left hemisphere), lip movement, tongue movement and vocalization (i.e. larynx activity during voice production) (*n* = 20). For vocalization, activation maxima in two separate brain areas were derived (dorsal and ventral larynx area).

Cortical surface maps of microstructural features

We derived whole-brain average surface maps for different measures related to cortical microstructure (Figure 5). Overall, the T1w/T2w map and the three MPM parameter maps (MPM_{MT}, MPM_{R1}, MPM_{R2*}) show a similar pattern of myelin content across the cortex (Figure 5**A**). In all four maps, the central sulcus as well as precentral and postcentral gyrus are characteristically high in myelin, which is considered to be a defining feature of primary motor and sensory cortex (Glasser and van Essen 2011) (Figure 5**B**). The location of the ventral boundary of the somatomotor cortex, indicated by a steep gradient of myelin values, slightly varies across the four maps, but this boundary is consistently more ventrally located in the right compared with the left hemisphere.

The fours maps that correlate with cortical myelin (T1w/T2w, MPM_{MT}, MPM_{R1} and MPM_{R2*}) are sensitive to different biophysical properties of the myelin, but it should be noted that their sensitivity profiles are not completely independent (Callaghan et al. 2016). Therefore, some dissimilarities regarding the distribution of myelin along the cortex can be observed across the maps. MPM_{MT} and MPM_{R1} have a stronger signal in the frontal lobe compared to the T1w/T2w and the MPM_{R2*} map. In addition to myelin, the R2* signal is influenced by cortical properties such as iron content and calcium (Wu et al. 2009; Bagnato et al. 2018). For the T1w/Tw2 map, the underlying biophysical model is less well understood. The high R2* values in the ventral temporal lobe are likely a susceptibility artifact caused by signal loss at the air-tissue boundary.

In the cortical thickness map, a prominent strip of low values (i.e. thinner cortex) can be observed at the posterior bank of the central sulcus, indicating the location of primary sensory cortex (Fischl and Dale 2000) (Figure 5**B**). Cortical thickness values are high (i.e. thicker cortex) in the anterior bank of the central sulcus and in the precentral gyrus, which is indicating the location of primary motor cortex. In the cortical thickness map, the ventral boundary of primary sensory cortex can be determined by a sharp gradient at the level of the subcentral gyrus. The location of this boundary is comparable with the location described above in the other maps. The same hemispheric difference can be observed with the somatomotor boundary being located further ventrally in the right hemisphere.

The whole brain maps demonstrate that these cortical surface measures are informative about the cortical microstructure underlying our functional activation maxima, which we describe in

the next section. The result of the reconstructed MPM parameter maps *per se* is not a primary result of the paper.

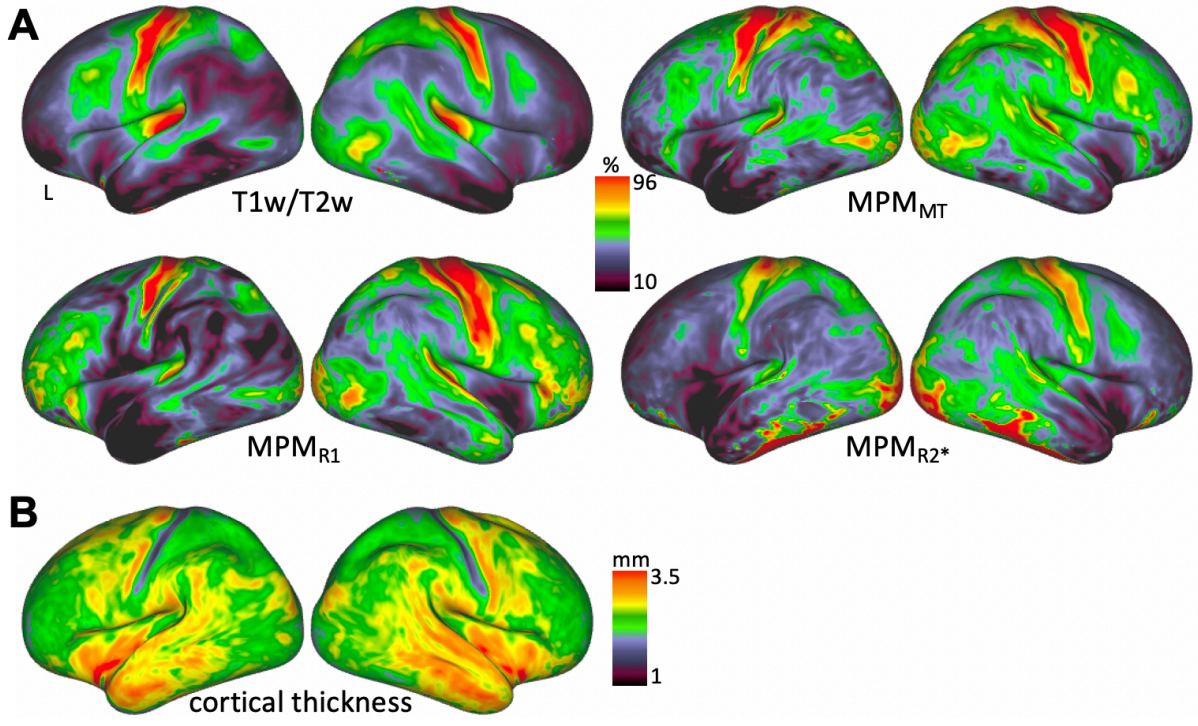

Figure 5 – Average cortical surface feature maps. **A**: T1w/T2w myelin map (*n* = 20) and MPM parameter maps (*n* = 19). **C**: Cortical thickness map (*n* = 20).

Microstructural properties at activation maxima

Next, we determined the intensity value of the microstructural surface maps at the individual subjects' activation maxima for the different movement types (Figure 6). Figure 6**A** shows z-transformed intensity values for T1w/T2w, MPM_{MT}, MPM_{R1} and MPM_{R2*} maps at hand, lip,

tongue as well as dorsal and ventral larynx maxima, i.e. at the peaks presented in Figure 4. Mixed effects analyses with the factors ROI (excluding the hand ROI), hemisphere and map demonstrated that there were highly significant effects of ROI ($F(3, 600) = 60.69$, $p < 0.001$) and hemisphere ($F(1, 600) = 43.54$, $p < 0.001$) but no significant effect of map ($F(3, 600) < 1$, *n.s.*). The significant effect of ROI reflects that values for the ventral larynx are lower than in the other ROIs (post-hoc pairwise *t*-tests with Tukey adjustment, $p < 0.001$), but the values for dorsal larynx area, lip and tongue were not significantly different. The main effect of hemisphere reflects higher values in the right hemisphere ($p < 0.001$). The interaction between ROI and hemisphere was significant ($F(3, 600) = 3.93$, $p = 0.009$) indicating that the difference between the ventral larynx area and the other areas was greater on the right hemisphere than on the left.

Cortical thickness values show a high inter-individual variability for hand, dorsal larynx, tongue and lip ROIs (Figure 6**B**). This effect can be attributed to the fact that some maxima are located in the depth of the central sulcus, where values are low, while others are located on the anterior bank of the central sulcus, where values are high. Variability in the right hemisphere is lower, which is consistent with the location of the maxima predominantly on the anterior bank (Figure 4). This result potentially indicates that some of derived maximal activation peaks represent activity evoked by somatosensation rather than by motor control. If maxima with a cortical thickness level below a cut-off value of 2 mm (Fischl and Dale 2000) are excluded, the comparison of cortical thickness values shows a marginally nonsignificant effect of ROI ($F(3, 120) = 2.53$, $p < 0.061$), but not of hemisphere ($F(1, 120) < 1$). The marginal effect of ROI is driven by the ventral larynx area having lower cortical thickness values compared to the other ROIs ($p < 0.068$).

To increase sensitivity in the quantification of myelin values described above, we re-ran the linear mixed model while excluding the sensory activation maxima as defined by a cortical thickness below 2 mm. The significant main effects of ROI ($F(3, 480) = 73.62$, $p < 0.001$) and hemisphere ($F(1, 480) = 20.81$, $p < 0.001$) were stronger than reported above. As reported above, the main effect of ROI is due to decreased values in the ventral larynx area and the hemispheric effect due to increased values in the right hemisphere. The interaction effect of ROI and hemisphere ($F(3, 480) = 2.26$, $p = 0.08$)) was no longer significant, indicating that the difference between ventral larynx area and the other areas did not differ between hemispheres.

To assess effects based on the non-transformed values of the four maps (T1w/T2w, MPM_{MT}, MPM_{R1}, MPM_{R2*}) rather than the *z*-scores, we also derived a 'dissimilarity matrix' based on the pair-wise Manhattan distances between ROIs after excluding the sensory activation maxima (Figure 6**C**). The values were averaged across hemispheres, because no significant interaction effect was found. The dissimilarity matrix reflects the effect of the ventral larynx area being most dissimilar from the other ROIs based on these quantitative measures of cortical myelin.

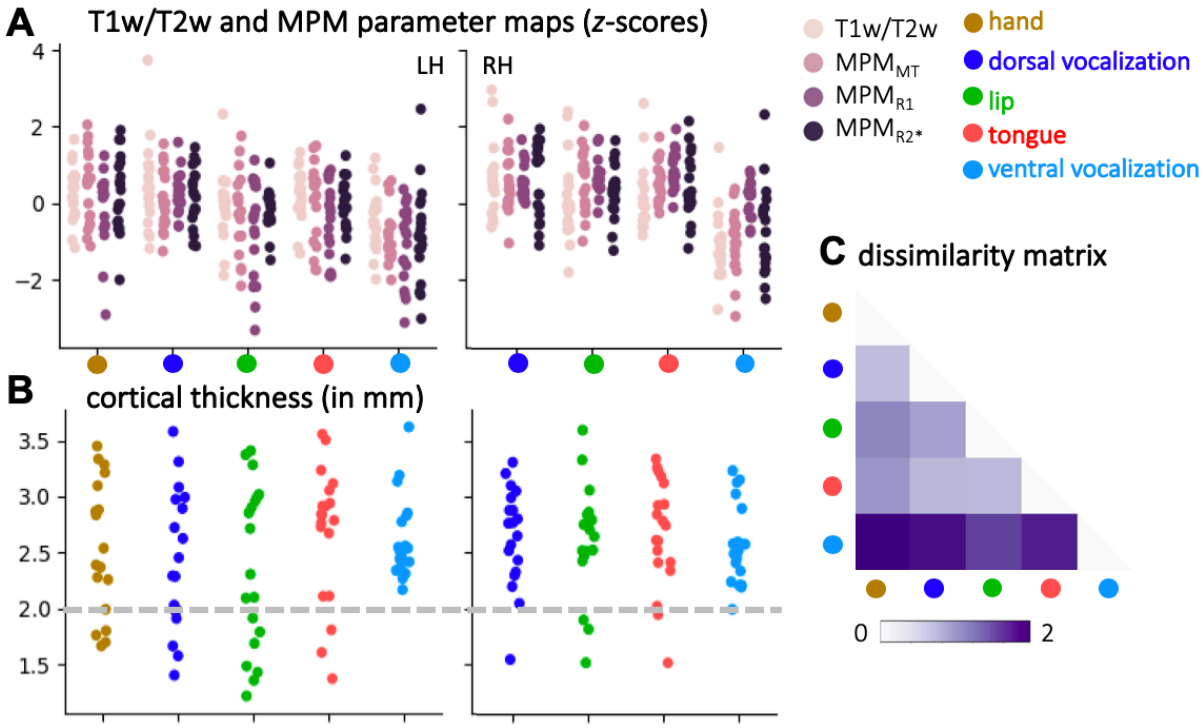

Figure 6 – Measures of cortical microstructure derived at individual activation maxima (n = 19). **A**: Microstructural values that correlate with myelin (T1w/T2w, MPM_{MT}, MPM_{R1}, MPM_{R2*}) derived at activation maxima (for individual maxima see Figure 4). **B**: Individual values of cortical thickness. The dashed grey line indicates the threshold that was chosen to determine the exclusion of activation maxima that are presumed to be sensory due to their location in cortex < 2 mm thick. **C**: Dissimilarity matrix of the myelin values across ROIs. The matrix shows a quantitative comparison of the values shown in **A** after excluding sensory activation maxima. Pair-wise dissimilarity is defined as the Manhattan distance between each pair of ROIs.

A linear discriminant analysis (LDA) revealed that the following equation can be used to discriminate the ventral larynx area from the dorsal larynx area:

$$y = -0.28 \cdot T1w/T2w - 2.82 \cdot MPM_{MT} - 3.03 \cdot MPM_{R1} - 0.47 \cdot MPM_{R2*} - 1.19$$

When inputting the *z*-transformed values of the surface maps at a specific location, a resulting value of y > 0 indicates that the profile of values is more similar to the ventral larynx area than to the dorsal larynx area. The formula indicates that MPM_{MT} and MPM_{R1} are the most informative measures to discriminate the two larynx areas (largest weighting). The mean performance accuracy of the classifier is 0.94 (while 0.5 indicates chance level performance).

Taken together, these quantifications show that the ventral larynx area is located in cortex that has lower myelin content and lower cortical thickness compared to primary motor cortex, where the other movement representations are located.

4. Discussion

The goal of this study was to localize brain activity evoked by voluntary control of laryngeal movements during vocalization. A second goal was to characterize the underlying cortical microstructure of this laryngeal representation. We show that even when controlling for breathing, vocalization elicits brain activity in two separate parts of the somatomotor cortex: a dorsal area in the central sulcus and a ventral area close to the Sylvian fissure. On an individual level, the laryngeal activations and the activations during movement of hand, lips, and tongue show a consistent somatotopic arrangement. Characterization of cortical microstructure based on structural and quantitative MRI shows that the dorsal larynx area has a similar profile to other primary motor areas, while the ventral larynx area has lower myelin content and cortical thickness. These results suggest that the dorsal larynx area is the primary locus of laryngeal motor control in primary motor cortex, while the ventral larynx activity relates more to secondary activations in non-primary motor cortex.

Our experimental task was designed to separate laryngeal activity from that evoked by supralaryngeal articulation and breathing. We were able to dissociate the supralaryngeal and laryngeal components of syllable production using a factorial design and orthogonal task contrasts (Murphy et al. 1997). The vocalization contrast showed some residual activity in the tongue area. Using the neutral vowel schwa or glottal stops instead (Gick 2002; Loucks et al. 2007; Brown et al. 2008; Grabski et al. 2012; Belyk et al. 2018), however, might have caused pharynx activity that would have been more difficult to dissociate.

In addition to the syllable production task, we used a basic localizer task that involved movement of the lips, and tongue, and vowel production. Results of the localizer task were consistent with the syllable production task, but the results of the latter are statistically more robust. The areas activated for the articulation contrast overlap with the result of the tongue localizer, which is expected given that the syllables produced mainly rely on tongue movement. The areas activated for the vocalization contrast overlap with the result of the vowel production condition, but some differences could be observed. Residual tongue activity resulting from the vowel /i/ is more apparent in the vowel production condition, suggesting that this was better controlled for in the factorial design.

When studying vocalizations, control for breathing is essential given that human vocal speech sounds are mostly produced during exhalation. Several previous neuroimaging studies, however, did not control for breathing. Some previous studies used a 'breathing only' condition for comparison with vocalization (Loucks et al. 2007; Simonyan et al. 2009; Galgano et al. 2019), but a difference in activation of regions in motor cortex was not found consistently.

One likely explanation is that explicitly instructing subjects to exhale might engage laryngeal muscles in such a way that no difference to laryngeal activity during vocalization can be observed. In this study, the breathing pattern and rate were matched for all task conditions. Breathing was explicitly instructed on a screen and monitored using a breath belt. Although slight deviations in the shape of the breathing trace can be observed, the overall breathing traces were comparable across subjects and conditions. The deviations in breathing patterns observed in the basic localizer task suggest that breathing is less well controlled for compared with breathing during the syllable production task, where subjects produced the same utterance in different conditions.

Our results suggest that controversial findings within the neuroimaging literature can largely be explained by differences in experimental design. Several studies focused on the dorsal region as location of the 'laryngeal motor cortex' or 'larynx phonation area' (Sörös et al. 2006; Brown et al. 2008; Kleber et al. 2013; Belyk and Brown 2014; Belyk et al. 2018). Brown et al. (2008) suggested the presence of a 'dorsolateral' larynx area on the crown of the precentral gyrus and a 'ventromedial' larynx area in the central sulcus. Our results suggest, however, that activity in the dorsal precentral area is a residual breathing-related signal and not specific for laryngeal activity during vocalization. In the 'breathing only' condition, we found activity in this precentral area, which is presumably related to control of the diaphragm (see Figure S1) (Ramsay et al. 1993; Olthoff et al. 2008). We also find this precentral activity during vowel production, but only when we use a resting condition as baseline (see Figure S1). When we subtract the 'breathing only' activity from the 'vowel production' activity, only the central dorsal larynx activation (in the sulcus) remains. A similar effect can be observed for the other task conditions, when the activity is compared to a resting baseline instead of controlling for

818 breathing. The activation that Brown et al. (2008) refer to as 'ventromedial' larynx area,
819 overlaps with the region that we describe here as dorsal larynx area in the central sulcus.
820
821 In addition to activity in the dorsal larynx area, multiple neuroimaging studies reported
822 activation in a region that we refer to as ventral larynx area (Terumitsu et al. 2006; Olthoff et
823 al. 2008; Grabski et al. 2012). Strong evidence for the involvement of a ventral larynx area in
824 laryngeal motor control also comes from electrical recording from the cortical surface during
825 vocalization and microsimulation studies (Galgano and Froud 2008; Bouchard et al. 2013;
826 Chang et al. 2013; Breshears et al. 2015; Dichter et al. 2018). Electrocorticography
827 demonstrated the presence of both a dorsal and a ventral larynx area much more consistently
828 than the fMRI literature (reviewed in Conant et al., 2014). Direct electrical stimulation of the
829 dorsal larynx area causes vertical larynx movement that correlates with stimulation magnitude
830 and evokes vocalization (Dichter et al. 2018); stimulation of the ventral larynx area causes
831 speech arrest (Chang et al. 2017).
832
833 In addition to our novel experimental design, this study focuses on investigating individual
834 differences in laryngeal activation patterns. The task count maps demonstrate that laryngeal
835 activity is much less consistent across subjects compared with other movement types. In some
836 subjects the dorsal or ventral activity did not reach the individual significance threshold. The
837 location of activation maxima in the ventral larynx area, in particular in the left hemisphere,
838 show a much wider spatial spread across the cortex indicating large intra-individual variability.
839 As a result of the variability and the low *z*-statistical values, group level fMRI analysis in previous
840 studies might have failed to detect one of the larynx areas. It remains to be investigated if the

variability in functional activation maxima is related to the underlying sulcal variability (Eichert et al. *in prep*).

The existence of two separate brain areas correlating with laryngeal activity in the central sulcus raises the question as to whether both of them are involved in motor control of the larynx. Given that the larynx area in the macaque is located in a ventral premotor area (Hast et al. 1974; Jürgens 1974; Simonyan and Jürgens 2002; Coudé et al. 2011), an evolutionary 'migration and duplication' hypothesis has been proposed (Belyk and Brown, 2017; Jarvis, 2019; reviewed in Mars et al., 2018). The theory states that the human ventral larynx migrated posteriorly during evolution, possibly into a different cytoarchitectonic area. The dorsal larynx area is thought to have evolved as human novelty in primary motor cortex.

Additional support for a duplication theory also comes from genetic profiling analyses comparing gene expressions in song-learning birds and humans (Pfenning et al. 2014; Chakraborty and Jarvis 2015). Gene expression in the avian vocal nuclei, that are involved in vocal learning, are similar to the expression profiles in both the dorsal and the ventral larynx areas of the human brain. In the context of this more general brain pathway duplication theory, it has been recently suggested that there was an additional duplication in human vocal premotor cortex, leading to the emergence of a pre-larynx motor cortex (preLMC) area just anterior to the ventral larynx area (Jarvis 2019). The proposed genetic mechanisms for the evolutionary brain pathway duplication theory in laryngeal motor control, however, remain to be verified experimentally.

The present study is the first to characterize the microstructural properties of cortex underlying the dorsal and ventral larynx area. The use of high-resolution quantitative neuroimaging allows us to characterize cortical architecture noninvasively (Weiskopf et al. 2013; Lutti et al. 2014). Measures from T1w/T2w maps and MPM parameter maps (MPM_{MT}, MPM_{R1}, MPM_{R2*}) are sensitive to different microstructural properties of the cortex, but all of them have been shown to correlate with myelin to varying degrees (Glasser and van Essen 2011; Weiskopf et al. 2013; Callaghan et al. 2014, 2015; Bagnato et al. 2018). Our quantification suggests strongly that the dorsal larynx area is located in primary motor cortex, which is characterized by high myelin content and thicker cortex (Fischl and Dale 2000; Glasser and van Essen 2011). The ventral larynx area, however, has lower myelin content and thinner cortex indicating that it is located in a different cortical territory. These results point towards a homology of human ventral larynx area with the non-human primate larynx area, which is not in primary motor cortex (Hast et al. 1974; Jürgens 1974; Simonyan and Jürgens 2002; Coudé et al. 2011). It remains to be determined, however, which cytoarchitectonic area underlies the ventral larynx activity. Based on a cytoarchitectonic map of the human brain (Brodmann 1905), it can be speculated that the human ventral larynx area is located in Brodmann area (BA) BA 6 (premotor cortex), as is the non-human primate larynx area, or in BA 43 (secondary sensory cortex). A magnetoencephalography study showed that air-puff stimulation in the larynx evokes activity in a ventral area, which is in line with a sensory rather than a motor role of the ventral larynx area (Miyaji et al. 2014) but spatial localization in MEG data is imprecise so it remains to be seen whether this location maps on to that seen in our study.

The question regarding the distinct functional contributions of the two larynx areas during voice productions remains unanswered. Based on our results, we formulate a hypothesis regarding the causal role of the two laryngeal areas during voice production: We propose that, as for vocalizations in non-human primates, the ventral larynx area is involved in basic control of the vocal folds so that a vocal sound can be produced. Rapid adduction (tensioning) and abduction (relaxation) of the vocal folds at the onset and offset of a vocalization is primarily modulated by the intrinsic laryngeal muscles (Jürgens 1974; Simonyan and Jürgens 2003). Fine motor control, which is required for pitch modulations in human speech and singing, however, also relies on the vertical movement of the larynx within the trachea, which is mediated by the extrinsic muscles. We suggest that pitch control is facilitated by the dorsal larynx area, which is located in primary motor cortex (Kleber et al. 2013; Dichter et al. 2018; Finkel et al. 2019). Activity in both intrinsic and extrinsic laryngeal muscles, however, are tightly coupled and might not be controlled by distinct brain areas (Belyk and Brown 2014). Our hypothesis is in line with an evolutionary theory suggesting that the dorsal larynx area is unique to the human brain (Belyk and Brown 2017). Such a functional dissociation of dorsal and ventral larynx area during vocalization, however, still needs to be tested directly using, for example, non-invasive brain stimulation.

In sum, we used neuroimaging to localize neural activity related to laryngeal motor control during vocalization, while controlling for confounding factors such as breathing and supralaryngeal articulation. We found two activated areas for laryngeal activity during vocalization, which are in anatomically distinct brain areas. Quantification of cortical microstructure suggests that the dorsal area, but not the ventral area, is located in primary

motor cortex. It remains open, whether and how these two brain areas differentially contribute to laryngeal motor control.

Acknowledgements

N.E. is a Wellcome Trust Doctoral student in Neuroscience at the University of Oxford [203730/Z/16/Z]. The project was supported by the NIHR Oxford Health Biomedical Research Centre. The Wellcome Centre for Integrative Neuroimaging is supported by core funding from the Wellcome Trust [203139/Z/16/Z]. The work of R.B.M. is supported by the Biotechnology and Biological Sciences Research Council (BBSRC) UK [BB/N019814/1] and the Netherlands Organization for Scientific Research NWO [452-13-015]. The Authors would like to thank Martina Callaghan from University College London for the MPM sequence.

Code Availability

Upon acceptance of the manuscript, all processing code will be made available from the Wellcome Centre for Integrative Neuroimaging's GitLab at git.fmrib.ox.ac.uk/neichert/project_larynx. FSL tools, are available from fsl.fmrib.ox.ac.uk. Connectome Workbench is available at www.humanconnectome.org/software/connectome-workbench.html.

Supplementary Material

Surface count maps of all individual task contrasts

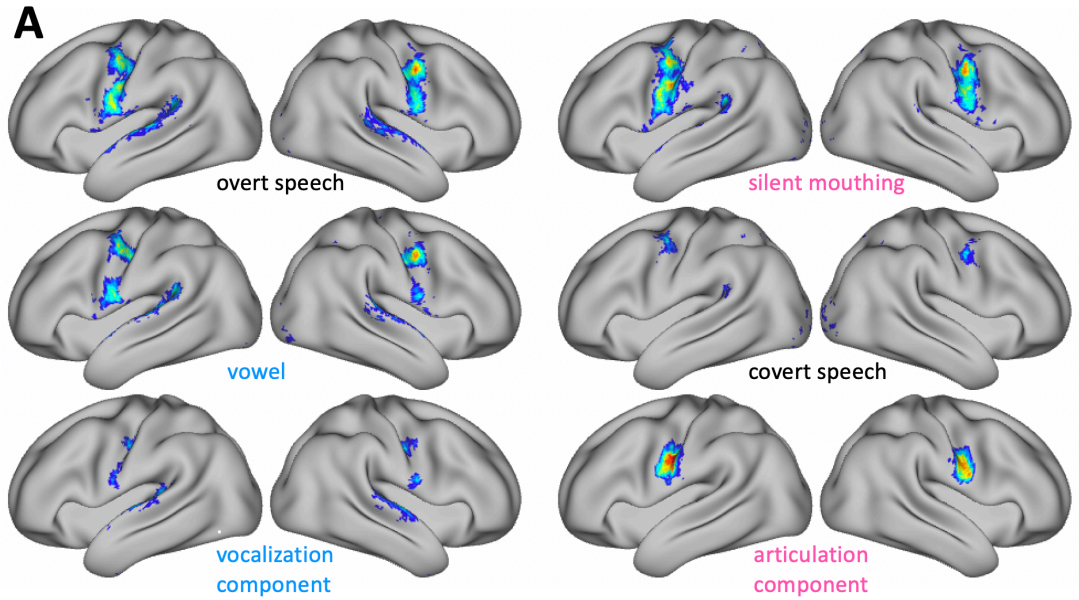

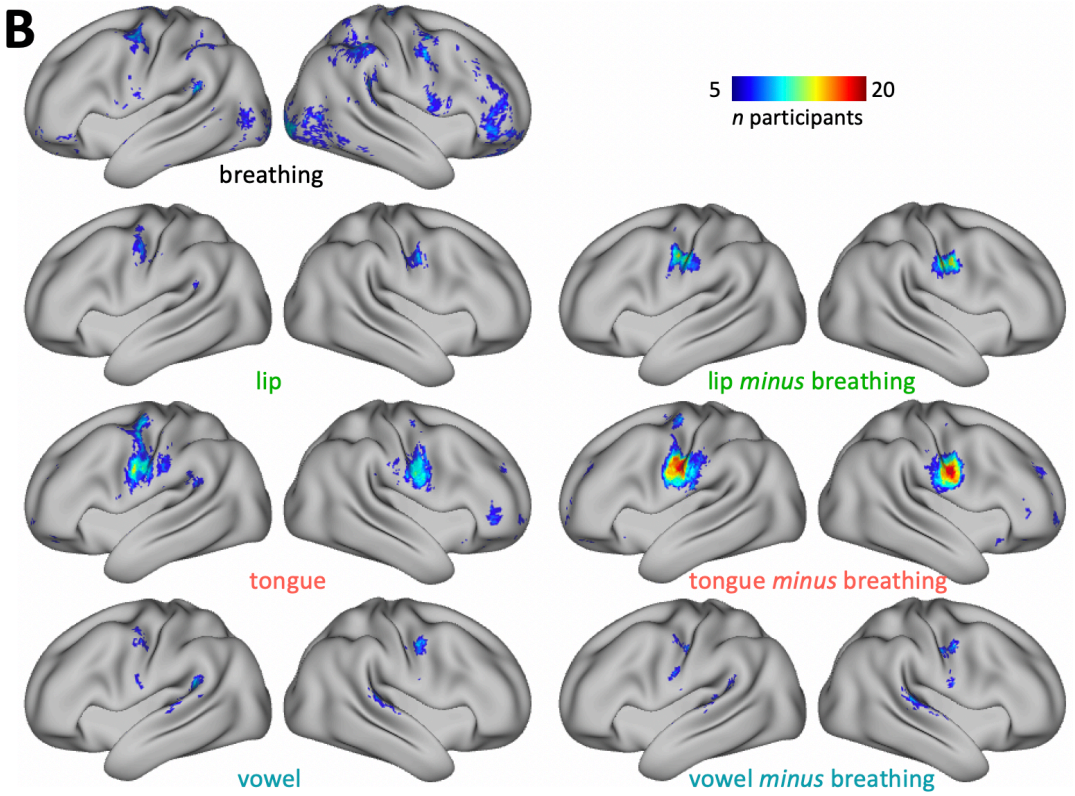

Figure S1 – Related to Figure 2 and Figure 3. Surface count maps of all individual task contrasts. **A**: Syllable production task: Four task conditions - overt speech, silent mouthing (articulation only), vowel production (vocalization only), covert speech (thinking) and two orthogonal contrasts for the articulation and vocalization component (the latter two are also shown in Figure 3B). **B**: Basic localizer task. Left panel: Task conditions compared to a resting baseline. For the 'breathing' condition a lower threshold of $z = 1.96$ was used to threshold individual *z*-statistical images due to generally lower activation. Right panel: Movement conditions compared to the breathing condition as baseline (also shown in Figure 2**B**).

Task activations in supplementary motor area

The two contrasts for articulation and vocalization - at a lower voxel-wise threshold of $z > 2$ - revealed activity bilaterally in SMA (Figure S2). A somatotopic arrangement was observed with vocalization activating a more anterior and more dorsal area. The representations of the effectors during the basic localizer task also show a clear somatotopy: In dorsal-to-ventral direction we first find the representation of the larynx, which is also most anterior, then of the lip and then of the tongue. Only one single representation of the larynx was found in SMA in both the 'vocalization' and the 'vowel' contrast.

The location of the representation of the speech effectors is in line with previous accounts in the literature (Picard and Strick 1996). It has been suggested that the vertical line crossing the anterior commissure, the VAC, is a landmark for a division of SMA proper and pre-SMA (Picard and Strick 1996; Rizzolatti et al. 1996). Our results thus suggest that lip and tongue representations are located just posterior to VAC in an anterior region of SMA proper. Laryngeal activity during vocalization, however, activates an area anterior to VAC, presumably in preSMA.

963

964 *Task activations in cerebellum*

965

966 Movement of the articulators and laryngeal activity also evoke activation of the cerebellum in
967 a somatotopic fashion, which is mirroring the order observed for motor cortex (Figure S2).
968 Most ventrally, a representation of the larynx is observed, which activates during vowel
969 production and vocalization. This is followed dorsally by a representation of the lips and the
970 tongue and then by a second representation of the larynx.

971

972 According to a probabilistic atlas of the human cerebellum (Diedrichsen et al. 2009), all the
973 activations observed are located in the anterior cerebellar lobule VI. This finding is consistent
974 with previous neuroimaging studies that found activation of the anterior-superior aspect of
975 cerebellum during speech movements (Petersen et al. 1989; Fiez and Raichle 1997). A previous
976 resting-state functional connectivity study demonstrated that cerebellar representations
977 mirror the topography in cerebral motor cortex (Buckner et al. 2011). It is therefore presumed
978 that the ventral-most laryngeal activation in cerebellum is a representation of the dorsal larynx
979 area in motor cortex and vice versa.

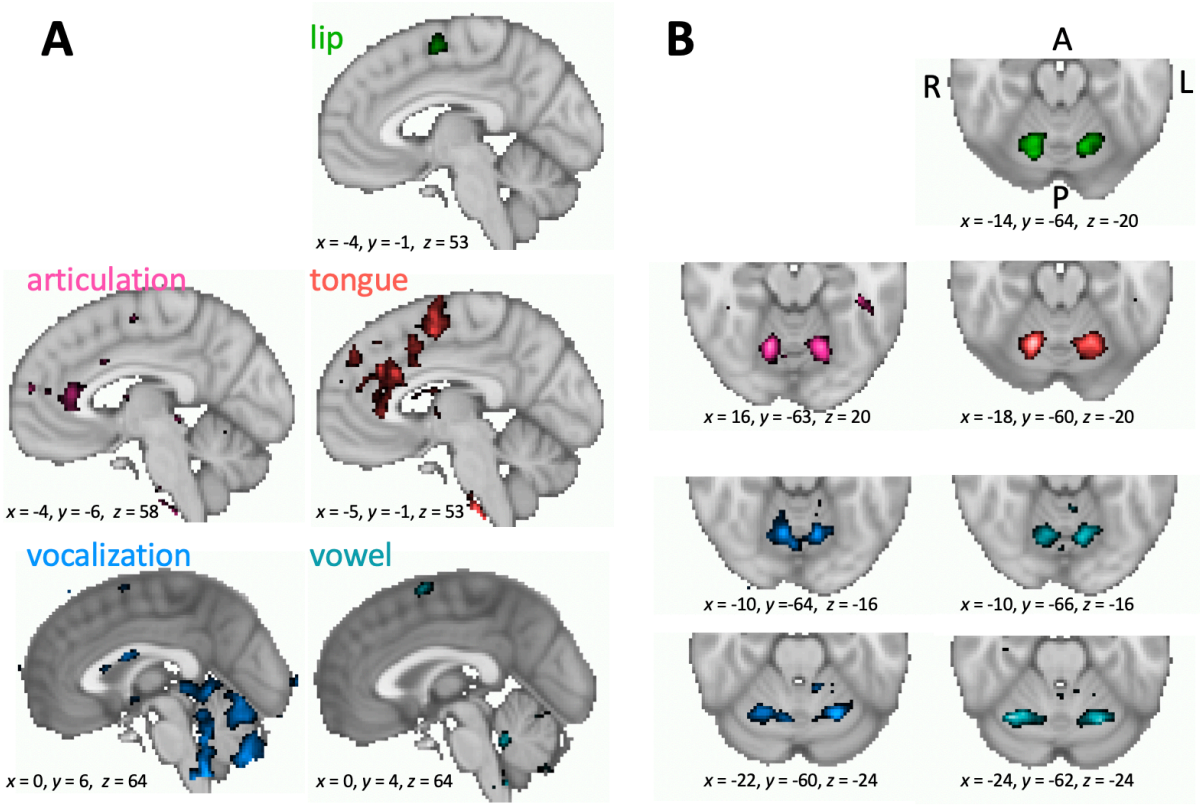

Figure S2 – Related to Figure 2 and Figure 3. Group activation maps showing areas activated during syllable production task (left panels) and basic localizer task (right panels) (vowel-wise threshold $z > 3.5$, $n = 20$). Coordinates are given for the voxel of maximal activation in the left hemisphere. **A**: Activity on the medial brain surface centered on the voxel of maximal activity in the left supplementary motor area (SMA) (note that for the 'vocalization' contrast the threshold was lowered to $z > 2$). **B**: Cerebellar activity in the same task contrasts and shown in the same colors as in **A**. For 'vocalization' and 'vowel' contrast, two separate activations are shown in different slices.

Regions-of-interest to derive maxima during task activation

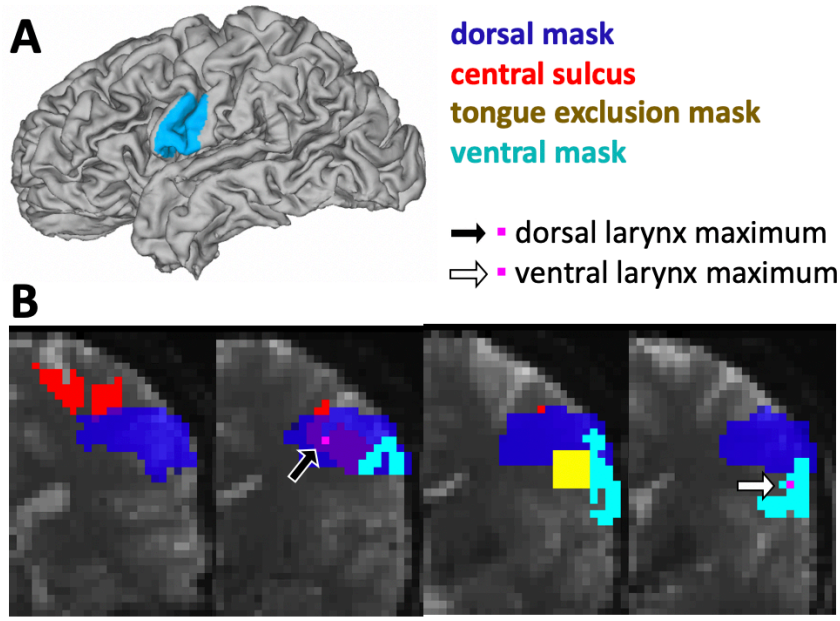

Figure S3 – Related to Methods. **A**: Example of a manually-drawn surface ROI for the ventral larynx area. The ROI was drawn on the individual's native surface and delineated anteriorly by the inferior precentral sulcus and posteriorly by the postcentral sulcus. **B**: Volumetric ROIs overlaid onto an individual's functional scan (coordinates for coronal sections refer to scanner anatomical space). The central sulcus ROI (red) was used to derive the voxel of maximal activation for the hand, lip and tongue. The intersection of the central sulcus ROI and a dorsal mask (dark blue, defined in MNI space z = 50 to z = 30) was used to derive the voxel of maximal activation for the dorsal larynx area (black arrow, pink voxel). The ventral mask was projected from surface to volume space (bright blue) to derive the voxel of maximal activation in the ventral larynx area (white arrow, pink voxel). A spherical ROI around the voxel of maximal activation in the tongue contrast was masked out from the dorsal and ventral mask (yellow).

1008 References

1009

1010 Ackermann H, Hage S, Ziegler W. 2014. Brain mechanisms of acoustic communication in
1011 humans and nonhuman primates: An evolutionary perspective. Behavioral and Brain
1012 Sciences. 37:529–604.
1013 Andersson JLR, Jenkinson M, Smith SM. 2007. Non-linear optimisation FMRIB technial eport
1014 TR07JA1.
1015 Bagnato F, Hametner S, Boyd E, Endmayr V, Shi Y, Ikonomidou V, Chen G, Pawate S,
1016 Lassmann H, Smith S, Brian Welch E. 2018. Untangling the R2* contrast in multiple
1017 sclerosis: A combined MRI-histology study at 7.0 Tesla. PLoS ONE. 13:e0193839.
1018 Barch DM, Burgess GC, Harms MP, Petersen SE, Schlaggar BL, Corbetta M, Glasser MF, Curtiss
1019 S, Dixit S, Feldt C, Nolan D, Bryant E, Hartley T, Footer O, Bjork JM, Poldrack R, Smith S,
1020 Johansen-Berg H, Snyder AZ, Van Essen DC. 2013. Function in the human connectome:
1021 Task-fMRI and individual differences in behavior. NeuroImage. 80:169–189.
1022 Bates DM, Sarkar D. 2007. Bates, Douglas M., and Deepayan Sarkar. "lme4: linear mixed-
1023 effects models using S4 classes. R package version 099875-6.
1024 Belyk M, Brown S. 2014. Somatotopy of the extrinsic laryngeal muscles in the human
1025 sensorimotor cortex. Behavioural Brain Research. 270:364–371.
1026 Belyk M, Brown S. 2017. The origins of the vocal brain in humans. Neuroscience and
1027 Biobehavioral Reviews. 77:177–193.
1028 Belyk M, Lee YS, Brown S. 2018. How does human motor cortex regulate vocal pitch in
1029 singers ? Royal Society Open Science. 5:172208.
1030 Bennett CM, Miller MB. 2010. How reliable are the results from functional magnetic
1031 resonance imaging? Annals of the New York Academy of Sciences.

Bohland JW, Guenther FH. 2006. An fMRI investigation of syllable sequence production. NeuroImage. 32:821–841.

Bouchard KE, Mesgarani N, Johnson K, Chang EF. 2013. Functional organization of human sensorimotor cortex for speech articulation. Nature. 495:327–332.

Breshears JD, Molinaro AM, Chang EF. 2015. A probabilistic map of the human ventral sensorimotor cortex using electrical stimulation. Journal of Neurosurgery. 123:340–349.

Brodmann K. 1905. Beitrage zur histologischen Lokalisation der Grosshirnrinde: III. Mitteilung. Die Rindenfelder der niederen Affen. J Psychol Neurol. 4:177–206.

Brown S, Laird AR, Pfordresher PQ, Thelen SM, Turkeltaub P, Liotti M. 2009. The somatotopy of speech: Phonation and articulation in the human motor cortex. Brain and Cognition. 70:31–41.

Brown S, Ngan E, Liotti M. 2008. A larynx area in the human motor cortex. Cerebral Cortex. 18:837–845.

Buckner RL, Krienen FM, Castellanos A, Diaz JC, Yeo BTT. 2011. The organization of the human cerebellum estimated by intrinsic functional connectivity. Journal of Neurophysiology. 106:2322–2345.

Callaghan MF, Freund P, Draganski B, Anderson E, Cappelletti M, Chowdhury R, Diedrichsen J, FitzGerald THB, Smittenaar P, Helms G, Lutti A, Weiskopf N. 2014. Widespread age-related differences in the human brain microstructure revealed by quantitative magnetic resonance imaging. Neurobiology of Aging. 35:1862–1872.

Callaghan MF, Helms G, Lutti A, Mohammadi S, Weiskopf N. 2015. A general linear relaxometry model of R1 using imaging data. Magnetic Resonance in Medicine. 73:1309–1314.

Callaghan MF, Mohammadi S, Weiskopf N. 2016. Synthetic quantitative MRI through

relaxometry modelling. NMR in Biomedicine. 29:1729–1738.

Carey D, Krishnan S, Callaghan MF, Sereno MI, Dick F. 2017. Functional and Quantitative MRI Mapping of Somatomotor Representations of Human Supralaryngeal Vocal Tract. Cerebral Cortex.

Casey BJ, Cannonier T, Conley MI, Cohen AO, Barch DM, Heitzeg MM, Soules ME, Teslovich T, Dellarco D V., Garavan H, Orr CA, Wager TD, Banich MT, Speer NK, Sutherland MT, Riedel MC, Dick AS, Bjork JM, Thomas KM, Chaarani B, Mejia MH, Hagler DJ, Daniela Cornejo M, Sicat CS, Harms MP, Dosenbach NUF, Rosenberg M, Earl E, Bartsch H, Watts R, Polimeni JR, Kuperman JM, Fair DA, Dale AM. 2018. The Adolescent Brain Cognitive Development (ABCD) study: Imaging acquisition across 21 sites. Developmental Cognitive Neuroscience. 32:43–54.

Chakraborty M, Jarvis ED. 2015. Brain evolution by brain pathway duplication. Philosophical transactions of the Royal Society of London Series B, Biological sciences. 370:20150056-.

Chang EF, Breshears JD, Raygor KP, Lau D, Molinaro AM, Berger MS. 2017. Stereotactic probability and variability of speech arrest and anomia sites during stimulation mapping of the language dominant hemisphere. Journal of Neurosurgery. 126:114–121.

Chang EF, Niziolek CA, Knight RT, Nagarajan SS, Houde JF. 2013. Human cortical sensorimotor network underlying feedback control of vocal pitch. Proceedings of the National Academy of Sciences. 110:2653–2658.

Conant D, Bouchard KE, Chang EF. 2014. Speech map in the human ventral sensory-motor cortex. Current Opinion in Neurobiology. 24:63–67.

Coudé G, Ferrari PF, Rodà F, Maranesi M, Borelli E, Veroni V, Monti F, Rozzi S, Fogassi L. 2011. Neurons controlling voluntary vocalization in the macaque ventral premotor cortex. PLoS ONE. 6:1–10.

Dichter BK, Breshears JD, Leonard MK, Chang EF. 2018. The Control of Vocal Pitch in Human Laryngeal Motor Cortex. Cell. 174:21-31.e9.

Diedrichsen J, Balsters JH, Flavell J, Cussans E, Ramnani N. 2009. A probabilistic MR atlas of the human cerebellum. NeuroImage. 46:39–46.

Draganski B, Ashburner J, Hutton C, Kherif F, Frackowiak RSJ, Helms G, Weiskopf N. 2011. Regional specificity of MRI contrast parameter changes in normal ageing revealed by voxel-based quantification (VBQ). NeuroImage. 55:1423–1434.

Fiez JA, Raichle ME. 1997. Linguistic Processing. In: International Review of Neurobiology. p. 233–254.

Finkel S, Veit R, Lotze M, Friberg A, Vuust P, Soekadar S, Birbaumer N, Kleber B. 2019. Intermittent theta burst stimulation over right somatosensory larynx cortex enhances vocal pitch-regulation in nonsingers. Human Brain Mapping. 1–14.

Fischl B. 2012. FreeSurfer. NeuroImage.

Fischl B, Dale AM. 2000. Measuring the thickness of the human cerebral cortex from magnetic resonance images. Proceedings of the National Academy of Sciences of the United States of America. 97:11050–11055.

Fitch WT. 2017. Empirical approaches to the study of language evolution. Psychonomic Bulletin and Review. 24:3–33.

Foerster O. 1936. Symptomatologie der Erkrankungen des Grosshirns. Motorische Felder und Bahnen. Sensible corticale Felder, Handbuch der Neurologie 6. Berlin: Springer.

Galgano J, Froud K. 2008. Evidence of the voice-related cortical potential: An electroencephalographic study. NeuroImage. 41:1313–1323.

Galgano J, Pantazatos S, Allen K, Yanagihara T, Hirsch J. 2019. Functional connectivity of PAG with core limbic system and laryngeal cortico-motor structures during human

phonation. Brain Research. 1707:184–189.

Gick B. 2002. An X-ray investigation of pharyngeal constriction in American English Schwa. Phonetica. 59:38–48.

Glasser MF, Goyal MS, Preuss TM, Raichle ME, Van Essen DC. 2014. Trends and properties of human cerebral cortex: Correlations with cortical myelin content. NeuroImage.

Glasser MF, Sotiropoulos SN, Wilson JA, Coalson TS, Fischl B, Andersson JL, Xu J, Jbabdi S, Webster M, Polimeni JR, Van Essen DC, Jenkinson M. 2013. The minimal preprocessing pipelines for the Human Connectome Project. NeuroImage. 80:105–124.

Glasser MF, van Essen DC. 2011. Mapping human cortical areas in vivo based on myelin content as revealed by T1- and T2-weighted MRI. Journal of Neuroscience. 31:11597–11616.

Grabski K, Lamalle L, Vilain C, Schwartz JL, Vallée N, Tropres I, Baciu M, Le Bas JF, Sato M. 2012. Functional MRI assessment of orofacial articulators: Neural correlates of lip, jaw, larynx, and tongue movements. Human Brain Mapping. 33:2306–2321.

Hast MH, Fischer JM, Wetzel AB, Thompson VE. 1974. Cortical motor representation of the laryngeal muscles in Macaca mulatta. Brain Research. 73:229–240.

Jarvis ED. 2019. Evolution of vocal learning and spoken language. Science. 366:50–54.

Jenkinson M. 2003. Fast, automated, N-dimensional phase-unwrapping algorithm. Magnetic Resonance in Medicine. 49:193–197.

Jenkinson M, Bannister P, Brady M, Smith S. 2002. Improved Optimization for the Robust and Accurate Linear Registration and Motion Correction of Brain Images Improved Optimization for the Robust and Accurate Linear Registration and Motion Correction of Brain Images. NeuroImage. 17:825–841.

Jenkinson M, Beckmann CF, Behrens TEJ, Woolrich MW, Smith SM. 2012. FSL. NeuroImage.

62:782–790.

Jenkinson M, Smith S. 2001. A global optimisation method for robust affine registration of brain images. Medical Image Analysis. 5:143–156.

Jürgens U. 1974. On the elicitability of vocalization from the cortical larynx area. Brain Research. 81:564–566.

Jürgens U. 2002. Neural pathways underlying vocal control. Neuroscience and Biobehavioral Reviews.

Kleber B, Zeitouni AG, Friberg A, Zatorre RJ. 2013. Experience-Dependent Modulation of Feedback Integration during Singing: Role of the Right Anterior Insula. Journal of Neuroscience. 33:6070–6080.

Kumar V, Croxson PL, Simonyan K. 2016. Structural Organization of the Laryngeal Motor Cortical Network and Its Implication for Evolution of Speech Production. Journal of Neuroscience. 36:4170–4181.

Leyton ASF, Sherrington CS. 1917. OBSERVATIONS ON THE EXCITABLE CORTEX OF THE CHIMPANZEE, ORANG-UTAN, AND GORILLA. Quarterly Journal of Experimental Physiology. 11:135–222.

Loucks TMJ, Poletto CJ, Simonyan K, Reynolds CL, Ludlow CL. 2007. Human brain activation during phonation and exhalation: Common volitional control for two upper airway functions. NeuroImage. 36:131–143.

Ludlow CL. 2005. Central nervous system control of the laryngeal muscles in humans. Respiratory Physiology and Neurobiology.

Lutti A, Dick F, Sereno MI, Weiskopf N. 2014. Using high-resolution quantitative mapping of R1 as an index of cortical myelination. NeuroImage. 93:176–188.

Lutti A, Hutton C, Finsterbusch J, Helms G, Weiskopf N. 2010. Optimization and validation of

1152 methods for mapping of the radiofrequency transmit field at 3T. Magnetic Resonance in
1153 Medicine. 64:229–238.
1154 Lutti A, Stadler J, Josephs O, Windischberger C, Speck O, Bernarding J, Hutton C, Weiskopf N.
1155 2012. Robust and fast whole brain mapping of the RF transmit field B1 at 7T. PLoS ONE.
1156 7:1–7.
1157 Mars RB, Eichert N, Jbabdi S, Verhagen L, Rushworth MFS. 2018. Connectivity and the search
1158 for specializations in the language-capable brain. Current Opinion in Behavioral
1159 Sciences. 21:19–26.
1160 McKay LC, Evans KC, Frackowiak RSJ, Corfield DR. 2003. Neural correlates of voluntary
1161 breathing in humans. Journal of Applied Physiology. 95:1170–1178.
1162 Miyaji H, Hironaga N, Umezaki T, Hagiwara K, Shigeto H, Sawatsubashi M, Tobimatsu S,
1163 Komune S. 2014. Neuromagnetic detection of the laryngeal area: Sensory-evoked fields
1164 to air-puff stimulation. NeuroImage. 88:162–169.
1165 Murphy K, Corfield DR, Guz A, Fink GR, Wise RJ, Harrison J, Adams L. 1997. Cerebral areas
1166 associated with motor control of speech in humans. Journal of applied physiology
1167 (Bethesda, Md : 1985). 83:1438–1447.
1168 Nieto-Castañón A, Fedorenko E. 2012. Subject-specific functional localizers increase
1169 sensitivity and functional resolution of multi-subject analyses. NeuroImage. 63:1646–
1170 1669.
1171 Olthoff A, Baudewig J, Kruse E, Dechent P. 2008. Cortical Sensorimotor Control in
1172 Vocalization: A Functional Magnetic Resonance Imaging Study. The Laryngoscope.
1173 118:2091–2096.
1174 Penfield W, Boldrey E. 1937. Somatic motor and sensory representation in the cerebral
1175 cortex of man as studied by electrical stimulation. Brain. 60:389–443.

Penfield W, Rasmussen T. 1950. The Cerebral Cortex of Man: Clinical Study of Localization of Function. Academic Medicine. 25:375.

Petersen SE, Fox PT, Posner MI, Mintun M, Raichle ME. 1989. Positron emission tomographic studies of the processing of single words. Journal of Cognitive Neuroscience. 1:153–170.

Pfenning AR, Hara E, Whitney O, Rivas M V, Wang R, Roulhac PL, Howard JT, Wirthlin M, Lovell P V, Ganapathy G, Mountcastle J, Moseley MA, Thompson JW, Soderblom EJ, Iriki A, Kato M, Gilbert MTP, Zhang G, Bakken T, Bongaarts A, Bernard A, Lein E, Mello C V, Hartemink AJ, Jarvis ED. 2014. Convergent transcriptional specializations in the brains of humans and song-learning birds. Science. 346:1256846–1256846.

Picard N, Strick PL. 1996. Motor areas of the medial wall: A review of their location and functional activation, Cerebral Cortex. Narnia.

Preibisch C, Deichmann R. 2009. Influence of RF spoiling on the stability and accuracy of T1 mapping based on spoiled FLASH with varying flip angles. Magnetic Resonance in Medicine. 61:125–135.

Ramsay SC, Adams L, Murphy K, Corfield DR, Grootoonk S, Bailey DL, Frackowiak RS, Guz A. 1993. Regional cerebral blood flow during volitional expiration in man: A comparison with volitional inspiration. The Journal of Physiology. 461:85–101.

Rizzolatti G, Luppino G, Matelli M. 1996. The classic supplementary motor area is formed by two independent areas. Advances in neurology. 70:45–56.

Simonyan K. 2014. The laryngeal motor cortex: Its organization and connectivity. Current Opinion in Neurobiology. 28:15–21.

Simonyan K, Jürgens U. 2002. Cortico-cortical projections of the motorcortical larynx area in the rhesus monkey. Brain Research. 949:23–31.

Simonyan K, Jürgens U. 2003. Efferent subcortical projections of the laryngeal motorcortex in

the rhesus monkey. Brain Research. 974:43–59.

Simonyan K, Ostuni J, Ludlow CL, Horwitz B. 2009. Functional But Not Structural Networks of the Human Laryngeal Motor Cortex Show Left Hemispheric Lateralization during Syllable But Not Breathing Production. Journal of Neuroscience. 29:14912–14923.

Smith SM. 2002. Fast robust automated brain extraction. Human Brain Mapping. 17:143–155.

Sörös P, Sokoloff LG, Bose A, McIntosh AR, Graham SJ, Stuss DT. 2006. Clustered functional MRI of overt speech production. NeuroImage. 32:376–387.

Tabelow K, Balteau E, Ashburner J, Callaghan MF, Draganski B, Helms G, Kherif F, Leutritz T, Lutti A, Phillips C, Reimer E, Ruthotto L, Seif M, Weiskopf N, Ziegler G, Mohammadi S. 2019. hMRI – A toolbox for quantitative MRI in neuroscience and clinical research. NeuroImage. 194:191–210.

Terumitsu M, Fujii Y, Suzuki K, Kwee IL, Nakada T. 2006. Human primary motor cortex shows hemispheric specialization for speech. Neuroreport. 17:1091–1095.

Toyoda G, Brown EC, Matsuzaki N, Kojima K, Nishida M, Asano E. 2014. Electrocorticographic correlates of overt articulation of 44 English phonemes: Intracranial recording in children with focal epilepsy. Clinical Neurophysiology. 125:1129–1137.

Weiskopf N, Callaghan MF, Josephs O, Lutti A, Mohammadi S. 2014. Estimating the apparent transverse relaxation time (R2*) from images with different contrasts (ESTATICS) reduces motion artifacts. Frontiers in Neuroscience. 8.

Weiskopf N, Suckling J, Williams G, Correia M. MM, Inkster B, Tait R, Ooi C, Bullmore T. ET, Lutti A. 2013. Quantitative multi-parameter mapping of R1, PD*, MT, and R2* at 3T: A multi-center validation. Frontiers in Neuroscience. 7:95.

Woo CW, Krishnan A, Wager TD. 2014. Cluster-extent based thresholding in fMRI analyses:

1224 Pitfalls and recommendations. NeuroImage. 91:412–419.

1225 Woolrich MW, Behrens TEJ, Beckmann CF, Jenkinson M, Smith SM. 2004. Multilevel linear
1226 modelling for FMRI group analysis using Bayesian inference. NeuroImage. 21:1732–
1227 1747.

1228 Woolrich MW, Ripley BD, Brady M, Smith SM. 2001. Temporal autocorrelation in univariate
1229 linear modeling of FMRI data. NeuroImage. 14:1370–1386.

1230 Wu Z, Mittal S, Kish K, Yu Y, Hu J, Haacke EM. 2009. Identification of calcification with MRI
1231 using susceptibility-weighted imaging: A case study. Journal of Magnetic Resonance
1232 Imaging. 29:177–182.

1233